IEEE Photonics Journal
An IEEE Photonics Society Publication

Open Access

Research on Three-Dimensional Magnetic Induced Error Model of Interferometric Fiber Optic Gyro

Volume 12, Number 5, October 2020

Zicheng Wang
Guochen Wang
Wei Gao
Zhuo Wang

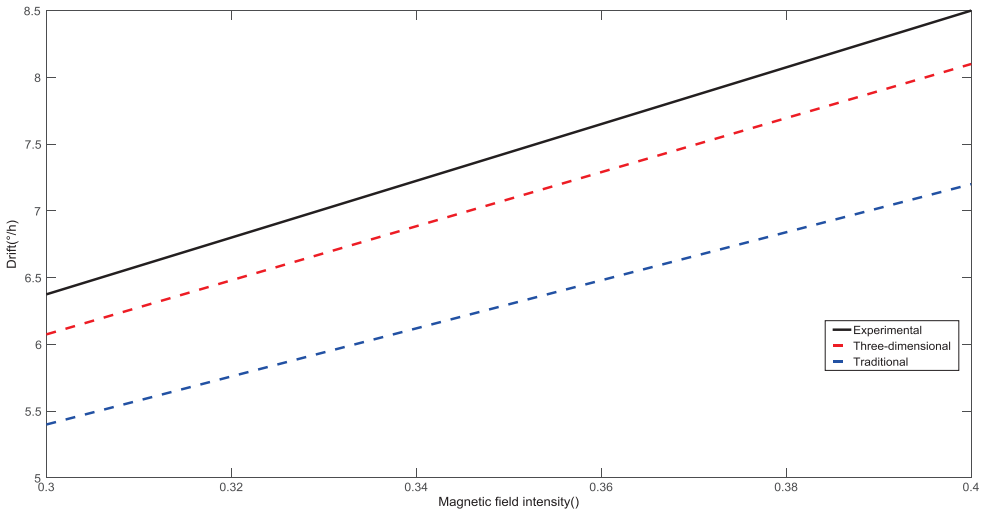

DOI: 10.1109/JPHOT.2020.3019059

IEEE photonics SOCIETY

IEEE

Research on Three-Dimensional Magnetic Induced Error Model of Interferometric Fiber Optic Gyro

Zicheng Wang, Guochen Wang, Wei Gao, and Zhuo Wang

Institute of Navigation Instruments, Harbin Institute of Technology, Harbin 150001, China

DOI:10.1109/JPHOT.2020.3019059

Manuscript received May 29, 2020; revised August 5, 2020; accepted August 20, 2020. Date of publication August 25, 2020; date of current version September 15, 2020. This work was supported in part by National Natural Science Foundation of China under Grant 51909048, in part by China Postdoctoral Science Foundation under Grants 2019T120260 and 2018M631920, and in part by Postdoctoral Foundation of Heilongjiang Province Government under Grants LBH-TZ1015 and LBH-Z17091. Corresponding author: Guochen Wang (e-mail: wanggc@hit.edu.cn).

Abstract: In practical, the Faraday effect-induced bias error is one of the main sources of bias error for the interferometric fiber optic gyroscope (IFOG). The Faraday effect-induced bias error impairs in the performance of IFOG. Normally, the Faraday effect-induced bias errors is hardly eliminated. To improve the performance of IFOG, the accurate model of Faraday effect-induced bias errors is necessary for its practical applications. In this paper, from the perspective of the finite element method, we calculate Faraday effect-induced bias errors of the fiber coil by the three-dimensional model in the radial magnetic field, and the axial magnetic field. Comparing with the traditional model, the differences mainly come from the size, and direction of the magnetic field, including the differences of the twist ratio, and the bending rate of each layer. Using the Jones matrix, we derive the three-dimensional magnetic field error model, further more theoretical results are obtained by simulation. The experiment with a 1024 m PM fiber coil are performed, and the experimental results support these theoretical predictions.

Index Terms: Fiber optics sensors, IFOG, three-dimensional fiber coil model, Faraday effect-induced bias errors.

1. Introduction

Fiber optic gyro (FOG) is a core component of the third generation inertial measurement devices. It is widely used in military and civilian applications for its advantages of all solid state, high sensitivity, low cost and large dynamic range [1]–[7]. The principle of the interferometric fiber optic gyroscope (IFOG) is based on the phase change caused by the Sagnac effect. The working environment of FOG is complicated and affected by many physical factors. It is necessary to distinguish the Sagnac phase from the non-reciprocity drift caused by environmental factors, such as temperature, vibration and magnetic field [8]–[13]. The most of researches are mainly focused on the effect of temperature. While, the influence of magnetic field is another important factor for IFOG and the research on magnetic field is still on primary stage. The magnetic field will produce a Faraday effect-induced bias error on the fiber coil [14]–[16], and the drift is difficult to distinguish form rotation velocity.

Polarization-maintaining fiber (PMF) is used in the IFOG to reduce the non-reciprocity caused by the birefringence variation and the Faraday effect-induced bias error [17], [18]. However, the fiber presents the twist during the winding process, and the phase shift of magneto-optical Faraday

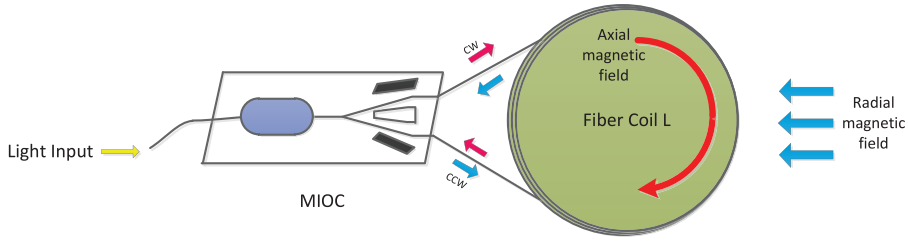

Fig. 1. IFOG optical path structure.

effect cannot be completely suppressed. In 2014, Liu *et al.* studied the magnetic sensitivity error of FOG under the radial magnetic field [19], and found that the torsion is the cause of the phase error. A method for suppressing the radial magnetic sensitivity was proposed by using the compensation fiber coil. The model was verified by experiments. The experimental results showed that compensation effect of the radial magnetic sensitivity reached 63.76% by using this fiber torsion compensation coil. In 2015, Zhang *et al.* proposed the research mechanism of the axial magnetic sensitivity of polarization-maintaining interferometric fiber optic gyro (PM-IFOG) for the first time [20].They proposed that the non-reciprocal phase difference generated by the axial magnetic field to PM-IFOG. For the fiber coil, the bending of the fiber is closely related to the twist distribution of the fiber. In 2017, the group of Li Xuyou, Li's research indicated that the residual Faraday effect-induced bias error of the PM-IFOG was about 1 °/h by 1Gs [21]. Magnetic shielding with high magnetic permeability allowed a magnetic induction coefficient of less than 0.01 °/h/Gs. The requirement can be achieved by using a magnetic shield of 30–40 dB. However, the magnetic shielding cannot completely isolate the magnetic field, and the Faraday effect-induced bias error still exists in the IFOG.

At present, the study of Faraday phase shift is based on two-dimensional model with a single-direction magnetic field in IFOG [22]–[25]. Actually, the IFOG is subjected to the radial magnetic field and the axial magnetic field simultaneously, so the single magnetic field cannot accurately calculate the Faraday effect-induced bias error under actual conditions. Moreover, the axial magnetic field and the radial magnetic field have different principle on the IFOG. The drift in the radial magnetic field is caused by the twist and Faraday effect-induced bias errors, and the drift in the axial magnetic field is caused by the change in the bending rate. In this paper, a three-dimensional Faraday error model is proposed. The finite element method is used to calculate the intensity of magnetic Faraday phase shift generated by the axial magnetic field and the radial magnetic field, respectively. The three-dimensional mathematical model of the fiber coil is built, and the simulation is carried out. The correctness of the three-dimensional Faraday magneto-offset theory is verified by the simulation and experiments.

2. Theory and Analysis

IFOG uses a closed-loop wideband modulation technique. Fig. 1 shows the diagram of optical path structure of IFOG. The optical routing is composed of light source, multifunction integrated optic circuit (MIOC), and fiber-optic coil. The MIOC is used for splitting, polarizing and phase-modulating [16], [26], [27]. The light source outputs light waves with wavelength stability and high power. The pigtail of MIOC is shorter than the 1024 m fiber optic coil, and the magneto-optical Faraday effect can be ignored. Therefore, the influence of magnetic field affects mainly on the fiber coil [1], [20]. In this paper, the fiber coil is considered as a three-dimensional model. Magnetic field is divided into the radial magnetic field and the axial magnetic field to calculate the Faraday effect-induced bias error.

2.1 Radial Magnetic Field

The principle of radial magnetic field is magneto-optical Faraday effect. Faraday produces different Faraday rotation angle when the intensity of magnetic field changes. Generally, the fiber coil cannot avoid the twist of fiber during the winding process, in which the twist changes the distribution of refractive index in the fast-axis and slow-axis. So there is a non-reciprocal phase difference between the clockwise (CW) direction and the counterclockwise (CCW) direction, which cannot be distinguished from the shift of Sagnac phase. The drift of each segment is calculated by the finite element method. Taking the fiber coil as a target, we take a small segment of PMF and assumed that r_{out} represents the outer radius, r_{in} indicates the inner radius. N, M, W, H and L denote the number of turn, the number of layer, the width of the coil, the height and the fiber coil of length, respectively.

The Jones matrix of light in CW direction direction is expressed as [23]

$$\mathrm{U}_{+} = \begin{bmatrix} \cos\eta_{+}dz - j\frac{\Delta\beta}{2\eta_{+}}dz & -\frac{\varepsilon_i+t_i}{\eta_{+}}\sin\eta_{+}dz \\ \frac{\varepsilon_i+t_i}{\eta_{+}}\sin\eta_{+}dz & \cos\eta_{+}dz + j\frac{\Delta\beta}{2\eta_{+}}\sin\eta_{+}dz \end{bmatrix} \tag{1}$$

Assuming that each piece of fiber with a length of dz is evenly distributed with $\eta_{+} = \sqrt{(\frac{\Delta\beta}{2})^2 + (\varepsilon_i + t_i)^2}$, $\Delta\beta$ is intrinsic linear birefringence. ε_i and t_i denote the circular birefringence caused by Faraday effect and twist, respectively. Here $\varepsilon_i = VB_r\sin(dz/r)$, V represents the Verdet constant of the fiber, B_r indicates radial magnetic intensity. Similarly

$$\mathrm{U}_{-} = \begin{bmatrix} \cos\eta_{-}dz - j\frac{\Delta\beta}{2\eta_{-}}dz & -\frac{\varepsilon_i+t_i}{\eta_{-}}\sin\eta_{-}dz \\ \frac{\varepsilon_i+t_i}{\eta_{-}}\sin\eta_{-}dz & \cos\eta_{-}dz + j\frac{\Delta\beta}{2\eta_{-}}\sin\eta_{-}dz \end{bmatrix} \tag{2}$$

The electric field vector of CW direction E_{+} and the electric field vector of CCW direction E_{-} can be expressed as [20]

$$E_{+} = \begin{bmatrix} 1 & 0 \\ 0 & 0 \end{bmatrix} \prod_{i=1}^{n} U_{+} \begin{bmatrix} 1 & 0 \\ 0 & 0 \end{bmatrix} E_0 \exp(-j\phi) \tag{3}$$

$$E_{-} = \begin{bmatrix} 1 & 0 \\ 0 & 0 \end{bmatrix} \prod_{i=1}^{n} U_{-} \begin{bmatrix} 1 & 0 \\ 0 & 0 \end{bmatrix} E_0 \tag{4}$$

where E_0 is initial electric field component in the fiber optic coil. The fiber coil is divided into n pieces, the length of the piece is $dz = L/n$ [24]. $\phi_{=}\phi_{\mathrm{s}} + \Delta\phi(t)$ contains the Sagnac phase shift ϕ_{s} and the modulation-induced phase $\Delta\phi(t)$. It is easy to note that the phase difference Φ_{F} is caused by the optical path difference between CW and CCW.

$$\Phi_{\mathrm{F}} = \frac{4V}{\Delta\beta}\int_0^L B_r(z)\sin\left(\frac{z}{r} - \theta\right)dz \tag{5}$$

where r represents the radius of fiber coil. So magnetically induced the drift of gyro is

$$\Omega_{\mathrm{F}} = \frac{\lambda cV}{\pi r\Delta\beta L}\int_0^L B_r(z)\sin\left(\frac{z}{r} - \theta\right)dz \tag{6}$$

where λ is the light wavelength; and c is the velocity of light in vacuum.

Fig. 3(a) shows the geometric relationship between the microelements and positions in the radial magnetic field. Fig. 3(b) shows the propagation of polarized light is affected by magnetic field. In ideal case, the Faraday effect-induced bias error is symmetrically distributed, which is the smallest in the parallel, and the largest in the perpendicular. In practice, due to the twist, the polarization axis has an angle with the magnetic field, which changes the Faraday effect-induced bias error. Define

$$M_{\mathrm{F}}(z) = \int_0^L B_r(z)\sin\left(\frac{z}{r} - \theta\right)dz \tag{7}$$

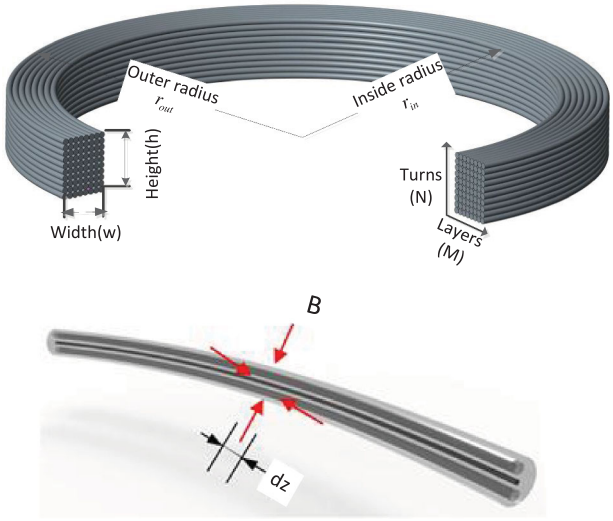

Fig. 2. Three-dimensional model of fiber coil and micro-decomposition of fiber coil.

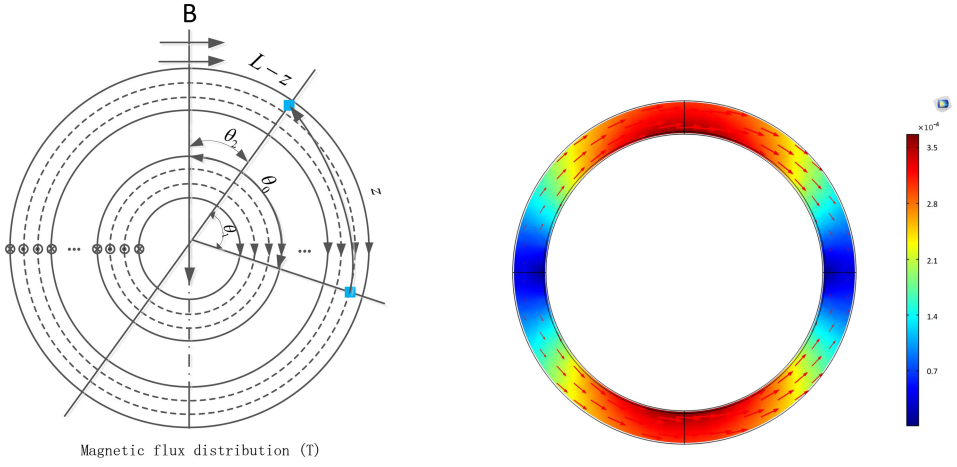

(a) Schematic diagram of fiber optic coil (b) Faraday effect simulation in COMSOL software

Fig. 3. Finite element simulation of radial magnetic model.

then

$$M_F(z) = \int_0^{\frac{L}{2}} B_r(z) \sin\left(\frac{z}{r} - \theta\right) dz + \int_{\frac{L}{2}}^{L} B_r(z) \sin\left(\frac{z}{r} - \theta\right) dz \tag{8}$$

Variable substitution for the second item

$$M_F(z) = \int_0^{\frac{L}{2}} B_r(z) \sin\left(\frac{z}{r} - \theta\right) dz + \int_0^{\frac{L}{2}} B_r(L - z) \sin\left(\frac{L - z}{r} - \theta\right) dz \tag{9}$$

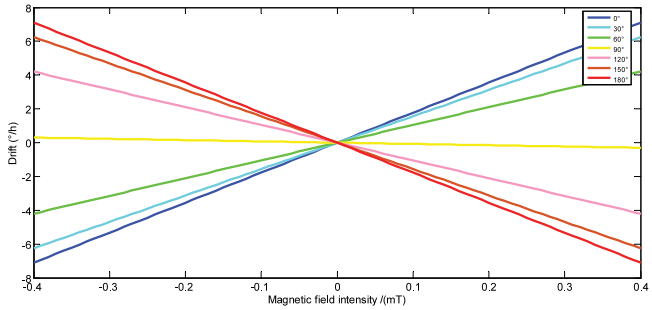

Fig. 4. The simulation result of radial magnetic field.

Different magnetic fields at different locations in the fiber optic coil, so

$$\begin{aligned} M_F(z) &= \sum_{k=1}^{N}\Big[\int_{L_{k,1}^{+}} B_r(z)\sin\left(\tfrac{z}{r}-\theta\right)dz + \int_{L_{k,2}^{+}} B_r(z)\sin\left(\tfrac{z}{r}-\theta\right)dz \\ &+\int_{L_{k,1}^{-}} B_r\left(L-z\right)\sin\left(\tfrac{L-z}{r}-\theta\right)dz + \int_{L_{k,2}^{-}} B_r\left(L-z\right)\sin\left(\tfrac{L-z}{r}-\theta\right)dz\Big] \\ &= \sum_{k=1}^{N}\Bigg[\sum_{j=1}^{M}\int_{L_{k,1}^{+j}} B_r(z)\sin\left(\tfrac{z}{r}-\theta\right)dz + \sum_{j=1}^{M}\int_{L_{k,2}^{+j}} B_r(z)\sin\left(\tfrac{z}{r}-\theta\right)dz \\ &+\sum_{j=1}^{M}\int_{L_{k,1}^{-j}} B_r\left(L-z\right)\sin\left(\tfrac{L-z}{r}-\theta\right)dz + \sum_{j=1}^{M}\int_{L_{k,2}^{-j}} B_r\left(L-z\right)\sin\left(\tfrac{L-z}{r}-\theta\right)dz\Bigg] \end{aligned} \tag{10}$$

where $B_r(z)$ and $B_r(L-z)$ are symmetrically distributed about the center $z=\frac{L}{2}$ of the fiber coil. L_k^j represents the position of micro-element. K and j recorded the number of layers and the number of turns, respectively. In the unit of fiber coil close to the inner diameter is denoted as $L_{k,1}$, and the outer diameter is denoted as $L_{k,2}$. In single-layer fiber, when $z<L/2$ is labeled $+$ and $z>L/2$ is labeled $-$. We ignore the attenuation of magnetic field by the polymer of fiber coil, $L_{k,1}$ and $L_{k,2}$ is tightly aligned fiber, then

$$\int_{L_k^{1,j}} dz = \int_{L_{k,1}^{+,j}} dz = \int_{L_{k,1}^{-,j}} dz \tag{11}$$

$$\int_{L_k^{2,j}} dz = \int_{L_{k,2}^{+,j}} dz = \int_{L_{k,2}^{-,j}} dz \ldots \int_{L_k^{n,j}} dz = \int_{L_{k,n}^{+,j}} dz = \int_{L_{k,n}^{-,j}} dz \tag{12}$$

The distribution of magnetic field obtained is only a function of the radial distance and the axial distance of the fiber coil. After the fiber is wound, the radius (r) and torsion rate of the coil (t_w) are fixed. Radial magnetic error is expressed as

$$\Omega_{Fr} = M\sum_{k=1}^{N}\frac{\lambda c V B_r}{\pi r \Delta\beta L}\int_0^{2\pi r} t_{w(z)}\sin(\frac{z}{r}-\theta)dz \tag{13}$$

M is denoted as the number of layer, and N is denoted as the number of turn. Radial magnetic error simulation is show in Fig. 4. The intensity of magnetic field increases linearly with the drift of IFOG. The magnetic field in different directions has different effects on the fiber coil. The drift of IFOG is the largest in 0 ° and 180 °, and the drift of IFOG is the smallest in 90 °.

2.2 Axial Magnetic Field

Two magnetic fields have different effects on the fiber coil. The fiber is bent after the winding of fiber coil (the radius of curvature is the radius of fiber coil). With the PMF in a bending state, the refractive index distribution always increases toward the center of curvature and decreases from

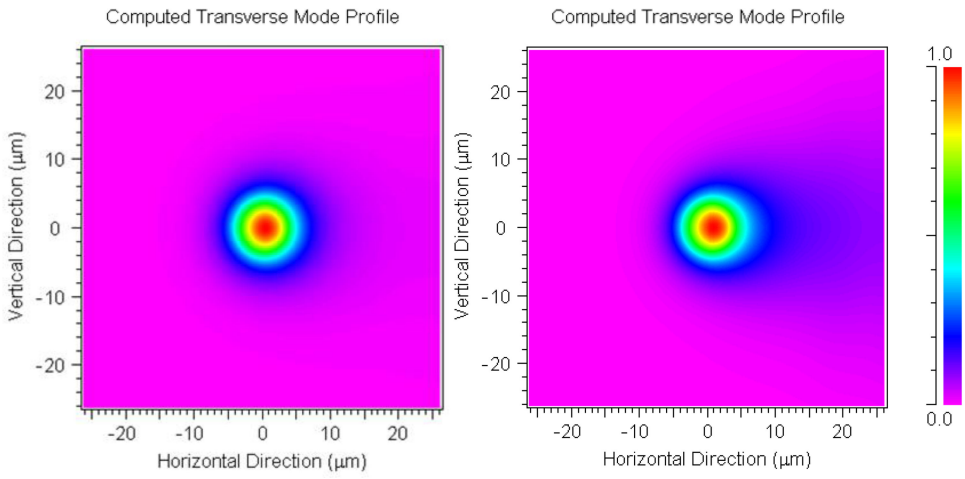

Fig. 5. Effect of fiber coil bending on birefringence.

the center side. This difference in refractive index distribution produces a polarization error for the light transmitting in the fiber, as shown in Fig. 5.

Light is split into two beams passing through the MIOC. The electric field component is $E_0 = [E_{0x}\ 0]^T$. The light of CW direction transmits through the optical path system, which is recorded as E_+. The light of CCW direction transmits through the optical path system, which is recorded as E_-. E_+ can be expressed as [14], [20]

$$\begin{aligned} E_+ &= \begin{bmatrix} E_{x+} \\ E_{y+} \end{bmatrix} = \begin{bmatrix} 1 & 0 \\ 0 & 0 \end{bmatrix} C_{q-M+,k} \cdots C_{q-M+,1} \begin{bmatrix} 1 & 0 \\ 0 & 0 \end{bmatrix} E_0 \\ &= \begin{bmatrix} 1 & 0 \\ 0 & 0 \end{bmatrix} \begin{bmatrix} \overline{A} & \overline{B} \\ -\overline{B}^* & \overline{A}^* \end{bmatrix} \begin{bmatrix} 1 & 0 \\ 0 & 0 \end{bmatrix} E_0 \\ &= E_x \begin{bmatrix} \cos\alpha\overline{A} + \sin\alpha\overline{B} \\ 0 \end{bmatrix} = E_x \begin{bmatrix} \cos\alpha A e^{-j\varphi_{A+}} + \sin\alpha B e^{j\varphi_{B+}} \\ 0 \end{bmatrix} \end{aligned} \tag{14}$$

where $\overline{A}$ and $\overline{B}$ are the amplitude of fast and slow axis transmission, respectively. φ_{A+} and φ_{B+} are the phase of fast and slow axis. α represents angle of incidence of light. Assuming that the Sagnac phase difference due to rotation is $\frac{\pi}{2}$, and the intensity of interference is modulated.The light intensity caused by the phase change of the two opposite beams is expressed as

$$\Delta I = 2E_{0x}^2(A\cos^2\alpha\sin(\varphi_s - \varphi_A) + B\sin^2\alpha\sin(\varphi_s + \varphi_B)) \tag{15}$$

When the fiber coil is subjected to axial magnetic field, the nonreciprocal phase caused by the axial magnetic field depends on the component of the polarized light in the direction of propagation. The change is roughly linear [28]. The derivation process is the similar to the case of radial magnetic field. Therefore, the axial magnetic field error model can be expressed as

$$\Omega_{Fa} = M\sum_{k=1}^{N}\frac{4VB_a n_{eff}(r)}{\Delta\beta}\int_0^{2\pi r} t_{w(z)}\frac{\cos^2\theta_i}{\pi}dz \tag{16}$$

where B_a represents the intensity of axis magnetic. $n_{eff}(r)$ denotes effective refractive index. The angle between the magnetic field and the fast axis of fiber indicates θ_i. Similarly,The simulation result of axial magnetic field is show in Fig. 6. The drift caused by the axial magnetic field and the

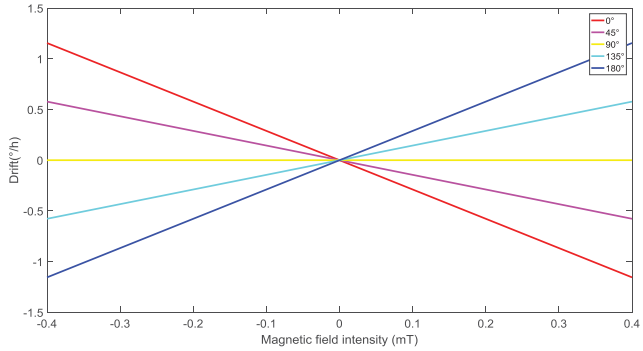

Fig. 6. The simulation result of axial magnetic field.

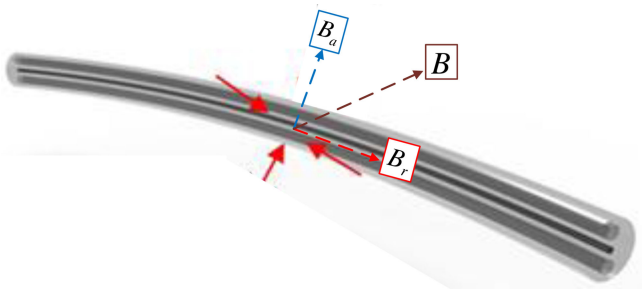

Fig. 7. Orthogonal decomposition of the magnetic field to fiber coil.

radial magnetic field are linear with the intensity of magnetic field, but on the value of zero drift is much smaller.

2.3 Three-Dimensional Magnetic Error Migration Model

Although both the radial and axial magnetic fields would cause phase errors, two magnetic fields have different effects on the fiber coil. The radial magnetic field produces elliptical birefringence with magneto-optical Faraday effect in the fiber, which results in optical path difference. The effect of axial magnetic field refers to the uneven of refractive index distribution caused by the bending of fiber coil. The magnetic field is a directional vector. In order to calculate Faraday effect-induced bias errors, we use the orthogonal method to decompose the magnetic field into an axial magnetic field and a radial magnetic field. When the fiber coil is affected by magnetic field, the magnetic field can be orthogonally decomposed into axial and radial magnetic fields as shown in Fig. 7. The magnetic errors caused by the axial and radial magnetic fields are superimposed to obtain a three-dimensional magnetic error model calculated from the number of layers and the number of turns from the inside to the outside. The model of three-dimensional magnetic Faraday effect-induced bias error can be expressed as

$$\Omega_F = M\sum_{k=1}^{N}\left[\frac{4VB_a n_{eff}(r)}{\Delta\beta}\int_0^{2\pi r} t_{w(z)}\frac{\cos^2\theta_i}{\pi}dz + \frac{\lambda cVB_r}{\pi r\Delta\beta L}\int_0^{2\pi r} t_{w(z)}\sin(\frac{z}{r}-\theta)dz\right] \tag{17}$$

The simulation results show that the Faraday effect-induced bias error of IFOG is the largest at 0 ° and 180 °, and the smallest at 90 °. Within a fixed angle, the relationship of the intensity of magnetic field is linear with the drift of IFOG.

TABLE 1
Fiber Coil Simulation Parameters

Parameter	Set value
Fiber coil length	1024m
Fiber diameter	165um
Number of layers	32
Number of turns	82
Fiber coil inner diameter	120mm
Fiber coil outer diameter	129.25mm
Light wavelength	1550nm
Verdet constant	0.84 rad/m/T
Intrinsic line birefringence	2027 rad/m

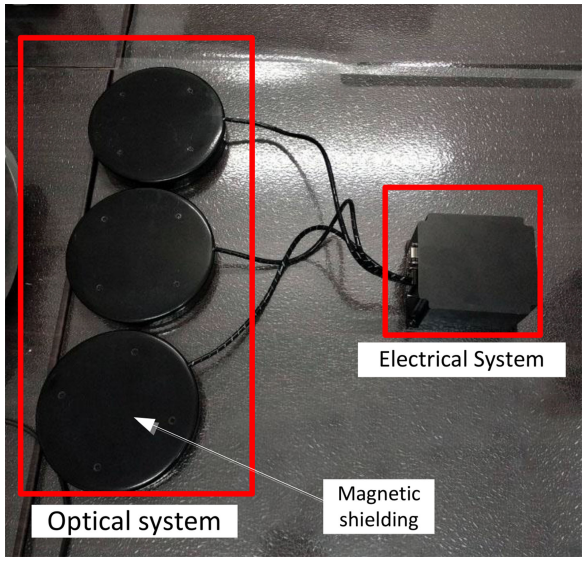

Fig. 8. Photoelectric separation structure.

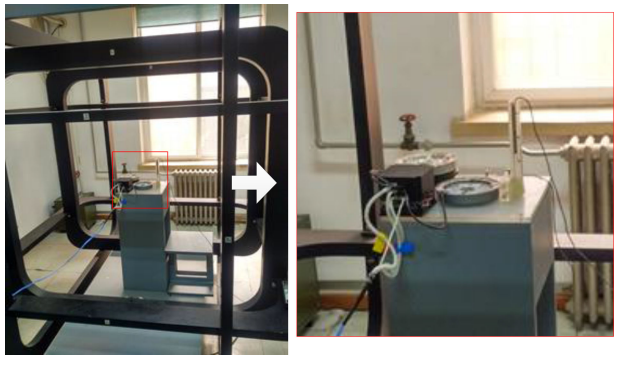

Fig. 9. The test platform and the Helmholtz coil radial magnetic field testing process.

3. Experiment and Result

To make the simulation more persuasive, three IFOGs are set on the experimental table according to Fig. 1. The parameters of IFOG are the same as those in Table 1. The system tests photoelectric separation structure that the light source and the optical fiber coil are divided into two independent spaces, as shown in Fig. 8. Fig. 9 presents the experimental systems.

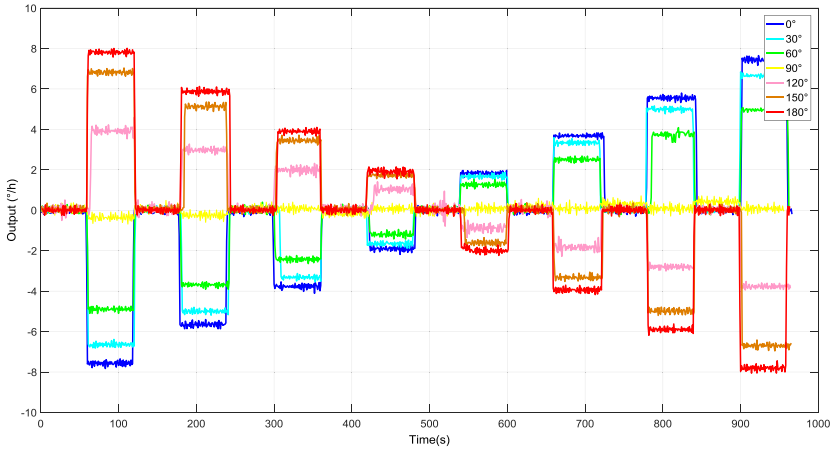

(a) the output data of IFOG A

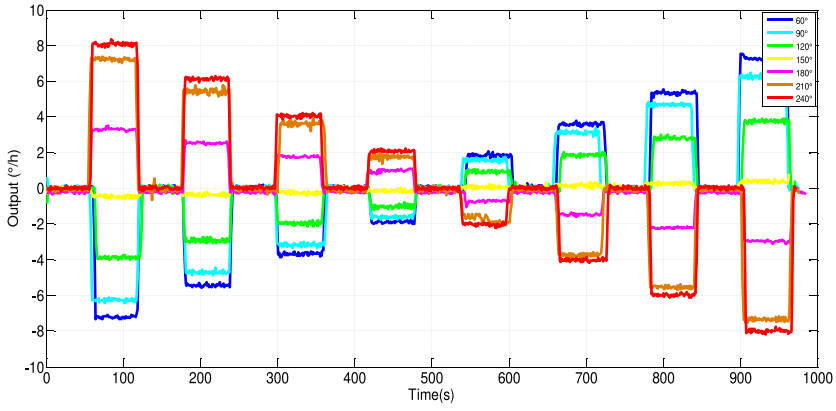

(b) the output data of IFOG B

Fig. 10. The experimental data of radial magnetic.

In order to get a uniform magnetic field, we build a Helmholtz coil to create a controllable magnetic field and ensure that the IFOG is located at the center of coil. The Helmholtz coil produces a uniform magnetic field at the center. The diameter of Helmholtz coil X-axis coil is 1899 mm, the diameter of Y-axis coil is 1640 mm, the diameter of Z-axis coil is 1769 mm. The intensity of magnetic field can be controlled by a current source and measured with a magnetic detection system. In order to reduce the device, the long side of Y waveguide is used as the reference, and the parallel direction is used as positive direction. Keeping the parameters of fiber coil unchanged, we change the angle between the radial magnetic field and IFOG, and record the output of IFOG [24]. The series magnetic field of 0.4 mT, 0.3 mT, 0.2 mT, 0.1 mT, 0 mT, -0.1 mT, -0.2 mT, -0.3 mT, -0.4 mT are applied from the radial direction by changing the intensity of coil current. The angle of the magnetic field changes in units of 30 degrees relatives to the direction of reference axis. The magnetometer reaches a steady state, and the output of IFOG is recorded in the each intensity of magnetic field. The data of IFOG is shown in Fig. 10.

The experimental method of the axial magnetic field is same as that of the radial direction. In each set of experiments, 0.4 mT, 0.3 mT, 0.2 mT, 0.1 mT, 0 mT, -0.1 mT, -0.2 mT, -0.3 mT, -0.4 mT intensity magnetic field are applied in the magnetic field. The data of IFOG is shown in Fig. 11. It can be seen from the principle that Faraday effect-induced bias error of the axial magnetic field is smaller, so the axial magnetic field changes the direction of IFOG and the X-axis in units of 45 degrees.

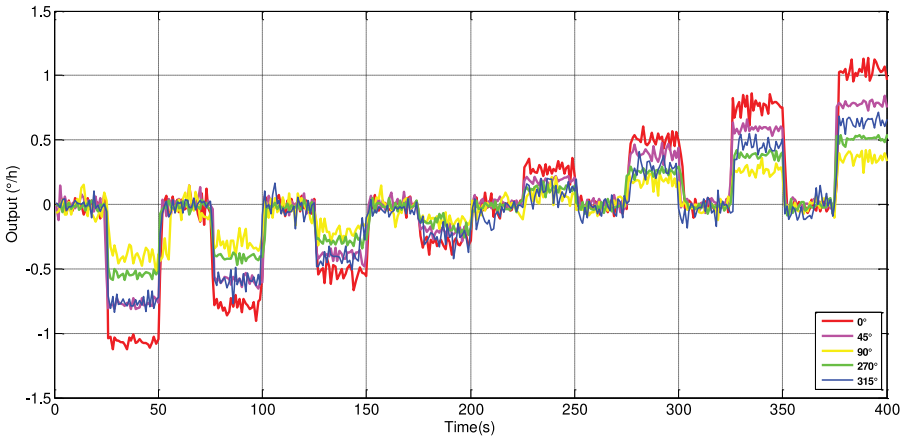

(a) the output data of IFOG A

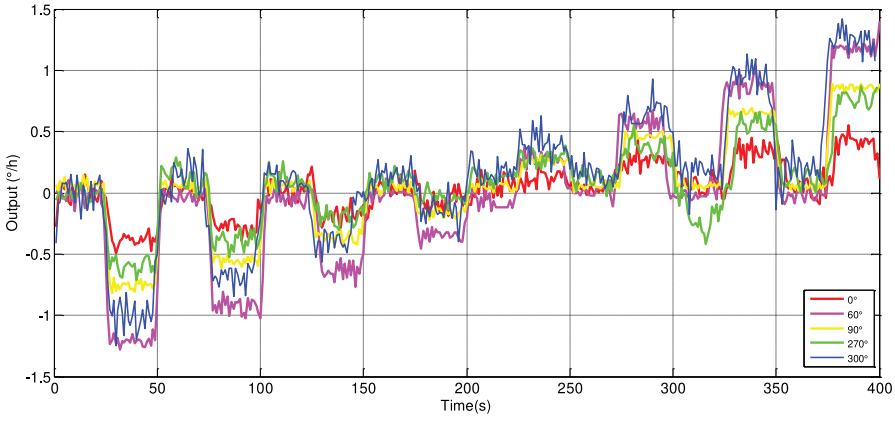

(b) the output data of IFOG B

Fig. 11. The experimental data of axial magnetic.

To make the experiment more accurate, the data of IFOG A, B, and C are simultaneously collected. The data is transmitted to computer for storage and offline processing. In the experiment, due to the angle between the fiber coil and the sensitive axis is different when IFOG is assembled, the angle of sensitive axis is 0 degrees in IFOG A, IFOGB is 30 degrees, and C is 60 degrees. In order to facilitate comparison, the article uses IFOG A as an example. By averaging the data, we find that the drift of IFOG is linear with the intensity of magnetic field. This is the same as theoretical simulation. Taking $\theta = 0^{\circ}$ as an example, the Faraday effect-induced bias errors increase linearly with the intensity of radial magnetic field and axial magnetic field, as shown in Fig. 12. As expected, the experimental results are completely consistent with theoretical predictions. We use Root Mean Square Error (RMSE) method to compare the experimental results with the simulation of two-dimensional model and three-dimensional model [21].

4. Discussion

It is noteworthy that the Faraday effect-induced bias errors are linear with the intensity of magnetic field when the direction of magnetic field is fixed with the angle of IFOG. When the intensity of magnetic field is constant, the Faraday effect-induced bias errors and the angle between the magnetic field and the fiber coil is sinusoidal relations. Both the radial magnetic field and the axial

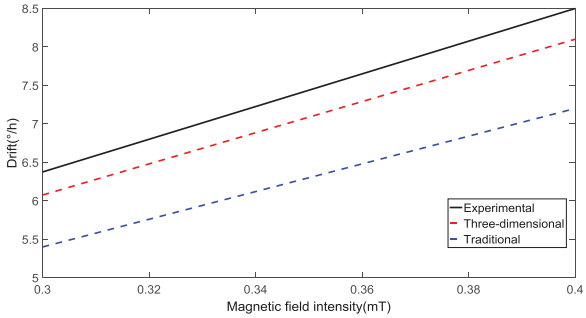

Fig. 12. Comparison of IFOG Faraday effect-induced bias errors results.

magnetic field conform to this principle, which is completely agreement with the theory. In Fig. 12, the experimental results are not exactly equal to the simulation results. During the experiment, we cannot put all the equipment into the thermostat. Due to the long experimental process, the temperature of surrounding has been changed. At the same time the IFOG produces heat from light source, PCB board which results in local temperature changes. According to the power (light source is 4.5 w, PCB board is 0.9 w) and material, we estimate the magnitude of Shupe Effect is 0.1–0.2°/h [29]. Moreover, in theoretical modeling, we used the average value of fiber twist, but the fiber twist is random in actual. The mathematical model of the random twist, through the refractive index and the four-pole symmetrical winding method of the fiber coil, can further improve Faraday effect-induced bias error model accuracy. In the other word, the drift can be suppressed with a dual-polarization optical structure. We can use the theory of Faraday effect to analyze the magnetic field and apply to design the structure of IFOG (increasing the thickness of magnetic shielding near the sensitive axis), which reduces the volume and the cost.

5. Conclusion

Using the finite element method, we established a three-dimensional error mathematical model of Faraday phase drift in IFOG. Different from the traditional method, we consider the Faraday effect-induced bias errors in different layers. Further, due to the different principle of magnetic field, we divide the magnetic field into radial and axial magnetic fields. Through simulation and experiment comparison, we find the intensity of magnetic field is linear with the output of IFOG when the angle between the magnetic field and the fiber coil does not change. When the intensity of magnetic field is constant, the angle is sinusoidal to the output of IFOG. The model of three-dimensional Faraday effect-induced bias error is obtained by combining the two errors, and the correctness is verified by experiments. While the fiber coil is surrounded by 0.4 mT magnetic field, the accuracy of Faraday effect-induced bias error model increased by 1.13°/h. We use the theoretical of the three-dimensional model and the traditional model to compare with the experimental results, respectively. The accuracy of the model is improved by 18.98%.

Acknowledgment

The authors would like to acknowledge Professor Jiubin Tan and all the staff in Navigation Instrument Research Institute for their technical support.

References

[1] X. Li, P. Liu, X. Guang, Z. Xu, L. Guan, and G. Li, “Temperature dependence of faraday effect-induced bias error in a fiber optic gyroscope,” *Sensors*, vol. 17, no. 9, 2017, Art. no. 2046.

[2] X. Li, S. Lin, J. Liang, Y. Zhang, H. Oigawa, and T. Ueda, "Fiber-optic temperature sensor based on difference of thermal expansion coefficient between fused silica and metallic materials," *IEEE Photon. J.*, vol. 4, no. 1, Feb. 2012.
[3] S. Pevec and D. Donlagic, "Multiparameter fiber-optic sensor for simultaneous measurement of thermal conductivity, pressure, refractive index, and temperature," *IEEE Photon. J.*, vol. 9, no. 1, Feb. 2017, Art. no. 2500114.
[4] Z. Wang *et al.*, "All-depolarized interferometric fiber-optic gyroscope based on optical compensation," *IEEE Photon. J.*, vol. 6, no. 1, Feb. 2014, Art. no. 7100208.
[5] Z. Li, N. He, X. Sun, C. Jin, C. Liu, and X. Wu, "Analysis of resonance asymmetry phenomenon in resonant fiber optic gyro," *Sensors*, vol. 18, no. 3, 2018, Art. no. 3390.
[6] H. Nie *et al.*, "Temperature stability of a hybrid polarization-maintaining photonic crystal fiber resonator and its application in a resonant fiber optic gyro," *Sensors*, vol. 18, no. 8, 2018, Art. no. 2506.
[7] G. A. Sanders, J. Wu, and M. Salit, "Fiber optic gyro development at honeywell," in *Proc. Spie Commercial + Scientific Sens. Imag.*, 2016, pp. 4–6.
[8] V. Vali and R. W. Shorthill, "Fiber ring interferometer," *Appl. Opt.*, vol. 15, no. 5, 1976, Art. no. 1099.
[9] D. Tazartes, "An historical perspective on inertial navigation systems," in *Proc. Int. Symp. Inertial Sensors Syst.*, 2014, pp. 318–883.
[10] G. A. Pavlath, "Fiber optic gyros past, present, and future," in *Proc. Ofs Int. Conf. Opt. Fiber Sensor*, 2012, vol. 8421, no. 2, pp. 1–10.
[11] J. N. Blake, "Magnetic field sensitivity of depolarized fiber optic gyros," *Proc. SPIE - The Int. Soc. Opt. Eng.*, vol. 1367, pp. 81–86, 1991.
[12] W. Zhou, Y. Zhou, X. Dong, L.-Y. Shao, J. Cheng, and J. Albert, "Fiber-optic curvature sensor based on cladding-mode Bragg grating excited by fiber multimode interferometer," *IEEE Photon. J.*, vol. 4, no. 3, Jun. 2012.
[13] P. Liu, X. Li, X. Guang, G. Li, and L. Guan, "Bias error caused by the faraday effect in fiber optical gyroscope with double sensitivity," *IEEE Photon. Technol. Lett.*, vol. 29, no. 15, pp. 1273–1276, Aug. 2017.
[14] Y. Zhao, Y. Zhou, D. Zhang, J. Yang, and L. Cheng, "Nonreciprocal phase error caused by orthogonal magnetic field in a polarization-maintaining fiber-optic gyro," *IEEE Sensors J.*, vol. 15, no. 9, pp. 5128–5132, Sep. 2015.
[15] Y. Zhao, D. Wu, R. Q. Lv, and J. Li, "Magnetic field measurement based on the sagnac interferometer with a ferrofluid-filled high-birefringence photonic crystal fiber," *IEEE Trans. Instrum. Meas.*, vol. 65, no. 6, pp. 1503–1507, Jun. 2016.
[16] V. N. Logozinskii, "Magnetically induced non-faraday nonreciprocity in a fiber-optic gyroscope," *J. Commun. Technol. Electron.*, vol. 51, no. 7, pp. 836–840, 2006.
[17] X. Cheng, J. Liu, J. Yin, and J. Lu, "Research on the approach of restraining faraday effect of fiber optic gyroscope with twisting fiber reversely," *Proc. SPIE - The Int. Soc. Opt. Eng.*, vol. 9297, pp. 92 972K–92 972K–7, 2014.
[18] P. Kumar, J. Nayak, and T. Srinivas, "Effect of magnetic field on the performance of fiber optic gyroscope," *J. Opt.*, vol. 41, no. 4, pp. 231–234, 2012.
[19] J. Liu, C. Xiao, X. Pan, J. Yin, and J. Lu, "Research on inhibiting radial magnetic sensitivity of fiber-optic gyroscope," *Chin. J. Lasers*, vol. 241.5, pp. 181–187, 2015.
[20] C. N. Zhang, M. F. Yang, Y. X. Zhao, D. W. Zhang, X. W. Shu, and C. Liu, "Research on the axial magnetic characteristic in a polarization maintaining fiber optic gyroscope," *Acta Photonica Sinica*, vol. 44, no. 12, 2015, Art. no. 1206003.
[21] L. Pan, X. Li, X. Guang, Z. Xu, W. Ling, and H. Yang, "Drift suppression in a dual-polarization fiber optic gyroscope caused by the faraday effect," *Opt. Commun.*, vol. 394, pp. 122–128, 2017.
[22] N. Song, X. Wang, X. Xu, W. Cai, and C. Wu, "Measurement of the verdet constant of polarization-maintaining air-core photonic bandgap fiber," *Sensors*, vol. 17, no. 8, 2017, Art. no. 1899.
[23] K. Hotate and K. Tabe, "Drift of an optical fiber gyroscope caused by the Faraday effect: Influence of the earth's magnetic field," *Appl. Opt.*, vol. 25, no. 7, 1986, Art. no. 1086.
[24] Y. Zhou, Y. Zhao, D. Zhang, X. Shu, and S. Che, "A new optical method for suppressing radial magnetic error in a depolarized interference fiber optic gyroscope," *Scientific Rep.*, vol. 8, no. 1, 2018, Art. no. 1972.
[25] D. W. Zhang, X. W. Shu, X. D. Mou, and C. Liu, "Theoretical study on radial magnetic field in fiber-optic depolarized gyro," *J. Transcluction Technol.*, vol. 18, no. 4, pp. 867–870, 2005.
[26] Z. Zhuo, Y. Fei, S. Qian, Z. Zhuo, Y. Fei, and S. Qian, "Thermal-induced rate error of a fiber-optic gyroscope considering various defined factors," *Opt. Eng.*, vol. 56, no. 9, 2017, Art. no. 0971031-9.
[27] R. Luo, Y. Li, S. Deng, C. Peng, and Z. Li, "Effective suppression of residual coherent phase error in a dual-polarization fiber optic gyroscope," *Opt. Lett.*, vol. 43, no. 4, pp. 81–85, 2018.
[28] Y. Yi, W. Zinan, and L. Zhengbin, "Optically compensated dual-polarization interferometric fiber-optic gyroscope," *Opt. Lett.*, vol. 37, no. 14, 2012, Art. no. 2841.
[29] B. Osunluk, S. Ogut, and E. Ozbay, "Thermally induced bias errors for a fiber coil with practical quadrupole winding," in *Proc. IEEE Int. Symp. Inertial Sensors Syst. (INERTIAL)*, 2017, pp. 16–22.